Journal of Applied Electrochemistry **30**: 385–392, 2000.

Preparation of $Bi_{1-x}Sb_x$ films by electrodeposition

F. BESSE, C. BOULANGER* and J.M. LECUIRE
Laboratoire d'Electrochimie des Matériaux – UMR 7555, Université de Metz, Ile du Saulcy, 57045 Metz cedex, France
*(*author for correspondence, e-mail: boulang@ipc.sciences.univ-metz.fr; fax: +33 387 315460)*

Received 25 May 1999; accepted in revised form 12 October 1999

Key words: antimony bismuth alloys, electrodeposition, semiconductors, thin films

Abstract

A method has been developed to produce composition modulated $Bi_{1-x}Sb_x$ alloys by electrodeposition. The electrolyte which consists of NaCl 4 M and HCl 1 M (pH 0) in aqueous medium, allows codeposition of bismuth and antimony to be accomplished at room temperature on glassy carbon. The composition of the films, their crystal structure, morphology and resistivity were studied as a function of electrochemical parameters and bath composition. It is shown that the electrodeposits are monophasic and exhibit a polycrystalline state. The obtained alloys represent a continuous series of solid solution. The film composition is dependent on the applied current density. The electrical resistivity is of the order of 3–7 $\mu\Omega$ m.

1. Introduction

$Bi_{1-x}Sb_x$ alloys are very attractive materials for thermoelectric refrigeration at low temperature [1, 2]. These materials are generally synthesized by directional crystallisation techniques (recrystallization [3], travelling heating method [4]) or by mechanical alloying [5]. These techniques do not readily lend themselves to production of large area thermoelements. In contrast, electrodeposition is a simple and low cost preparation technique which has been successfully applied to production of semiconductive material films. For instance, binary and ternary chalcogenides can be easily developed [6–8]. Examples of cathodically synthesised antimony based semiconductors (InSb [9, 10], GaSb [11, 12]) are less common. However, antimony bismuth alloy deposits have been obtained in galvanostatic conditions in the presence of ethylenediaminetetracetic acid (EDTA or Trilon B) according to Povetkin et al. [13].

$Bi_{1-x}Sb_x$ alloys have different electrical transport behaviour depending on their antimony composition [14–18]. The aim of this work was to produce an antimony–bismuth alloy with the best semiconductor characteristics suitable for thermoelectric application by exploring two electrochemical processes (potentiostatic and galvanostatic deposition). The processes are based on the coreduction of bismuth and antimony salts in an aqueous medium containing complexing agents (chloride). Complexation brings the reduction potentials of Sb and Bi close to each other ($BiCl_4^-/Bi^\circ$ $E^\circ = 0.16$ V, $SbCl_4^-/Sb^\circ$ $E^\circ = 0.17$ V [19]), thus allowing codeposition in spite of the difference in the standard potentials ($E^\circ = 0.32$ V for BiO^+/Bi° and $E^\circ = 0.21$ V for SbO^+/Sb° [19]).

2. Voltammetric analytical study

2.1. *Experimental details*

Voltammetric experiments were carried out in a conventional three-electrode device in a thermostated cell (25 °C) and under an inert atmosphere (argon HP). Working electrode was a rotating vitreous carbon disc (3 mm dia., EM-EDI-CVJ, Radiometer). In standard conditions, the rate of rotation was 625 rpm. The electrochemical potentials of the working electrode were measured and expressed by reference to the aqueous KCl saturated calomel electrode (SCE). The counter electrode was a platinum wire. A computer driven Radiometer PGP 201 potentiostat/galvanostat was used for cyclic voltammetric analysis.

The electrolytic baths were prepared with deionized water. To ensure the stability and the solubility of antimony^{III} and bismuth^{III} solutions on the one hand and to compensate for the difference in deposition potentials the two components on the other hand, the optimised electrolyte was a chloride solution (NaCl) containing hydrochloric acid in order to form chloride complexes ($BiCl_4^-$ and $SbCl_4^-$).

The Sb^{III} solutions were prepared by dissolution of Sb_2O_3 in a 1 M hydrochloric solution with 4 M NaCl added. The Bi^{III} solutions were obtained in the same way by dissolution of $Bi(NO_3)_3$, 5 H_2O. The Bi^{III} and

Sb^{III} electrolyte mixtures were obtained from the above solutions and various |Sb|/|Bi| ratios were tested, ranging between 0.05 and 1.2. All reagents were from PROLABO p.a. grade. The solution concentrations were controlled by atomic absorption spectrometry AAS (Solar, Unicam 969).

2.2. *Results*

The behaviour of Bi^{III}, Sb^{III} and their mixtures was investigated using cyclic or linear voltammetry.

2.2.1. *Single solutions*

The cyclic voltammetric curves obtained with a Bi^{III} solution in chloride medium is shown in Figure 1(a). At potentials more negative than −275 mV, a reduction process occurs due to deposition of elementary Bi°. The X-ray diffraction pattern of the electrodeposited product confirms the formation of metal. For potentials between −300 and −600 mV, the cathodic current is independent of potential. The diffusion current increases with increasing Bi^{III} concentration in solution. A shift towards more negative potentials than −600 mV causes solvent reduction. The anodic peak ($E_{ap} = -200$ mV) corresponds to the redissolution of Bismuth. The coulombic efficiency may be determined as the ratio between the charge spent for stripping Bi (Q_a) and the total charge transferred during deposition (Q_c). The coulombic efficiencies ($\rho = Q_a/Q_c$) were found to be fairly constant with changes in the negative switching potentials ($90 \pm 1\%$). The cathodic charge excess is certainly due to formation of a nonperfectly adherent product on the electrode.

Figure 1(b) shows a voltammetric curve for a $SbCl_4^-$ solution. During a cathodic exploration, a reduction wave begins at −300 mV due to the electrodeposition of antimony metal. The solvent reduction occurs from about −600 mV. A reverse sweep causes the anodic antimony stripping at $E_{ap} = -135$ mV, a value higher than the observed potential for Bi°. Thus, the antimony system appears to be less reversible than the bismuth system in such an electrolyte. The black metallic product obtained after a cathodic scan and analysed by X-ray diffraction corresponds to elementary antimony. The cathodic (Q_c) and anodic (Q_a) charges are slightly different. The variation in the Q_a/Q_c ratio (93% for −450 mV, 91% for −500, 75% for −600 mV) can be interpreted on the basis of hydrogen formation for the most negative potentials, causing a nonadherent powder electrodeposit.

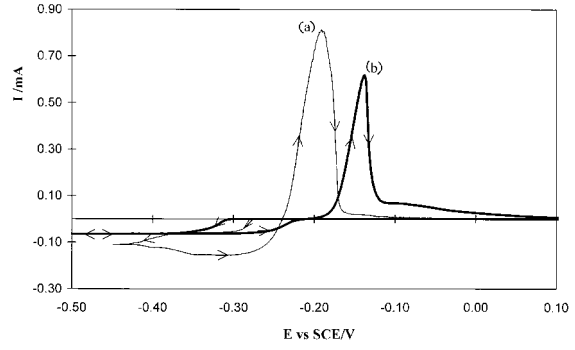

Fig. 1. Voltammogram in NaCl 4 M and HCl 1 M. Working electrode: glassy carbon; surface area: 7.06 mm^2, rotation rate: 625 rpm, scan rate: 60 mV min^{-1}. (a) $|Bi^{III}| = 10^{-3}$ M, (b) $|Sb^{III}| = 10^{-3}$ M.

2.2.2. *Mixtures solutions*

The similarity between the reduction potentials of $BiCl_4^-$ and $SbCl_4^-$ solutions and the quasi-equality of the equilibrium ($i = 0$) potentials of the two systems, allowing a possible electrodeposition of bismuth antimony alloys, led us to study solutions containing the two elements in different ratios. Therefore, we carried out deposition from solution with a Bi^{III} concentration maintained constant at 10^{-3} M and a Sb^{III} concentration varying from 0.05 to 1.2×10^{-3} M + NaCl 4 M + HCl 1 M at −450 mV for 2 min on a rotating glassy carbon electrode (described in Section 2.1). After deposition, the samples were submitted to stripping voltammetry. The voltammograms recorded in the same medium are presented in Figure 2.

All the curves show a reduction wave and one main stripping peak with a more or less marked shoulder at more positive potential. With the increasing antimony concentration, the reduction wave becomes higher and slighty shifts toward more positive ($E_{1/2}$ ranging between −250 and −200 mV). The position of the anodic peak between the specific signals of Bi° and Sb° is dependent on the Sb concentration, the increase in Sb^{III} concentration results in the shift of this peak in the anodic direction. The coulombic efficiencies, listed in the figure caption, are generally close to 90%. The curves show that the two elements (bismuth and antimony) are not oxidatively dissolved independently of one another.

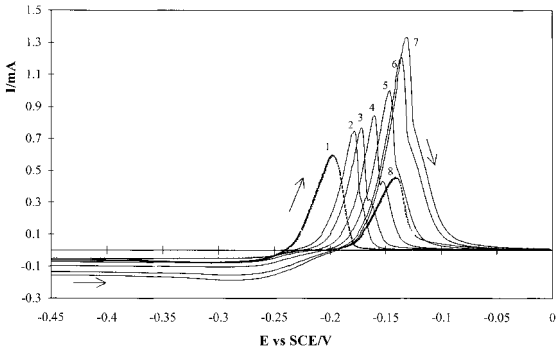

Fig. 2. Voltammogram in NaCl 4 M and HCl 1 M of Sb^{III} and Bi^{III} solutions. Working electrode: glassy carbon, surface area: 7.06 mm^2, rotation rate: 625 rpm, scan rate: 60 mV min^{-1} Curves: (1) $|Bi^{III}| = 10^{-3}$ M, $Q_a/Q_c = 90\%$; (2) $|Sb^{III}| = 5 \times 10^{-5}$ M, $|Bi^{III}| = 10^{-3}$ M, $|Sb^{III}|/|Bi^{III}| = 0.05$, $Q_a/Q_c = 83\%$; (3) $|Sb^{III}| = 10^{-4}$ M, $|Bi^{III}| = 10^{-3}$ M, $|Sb^{III}|/|Bi^{III}| = 0.1$, $Q_a/Q_c = 73\%$; (4) $|Sb^{III}| = 2.5 \times 10^{-4}$ M, $|Bi^{III}| = 10^{-3}$ M, $|Sb^{III}|/|Bi^{III}| = 0.25$, $Q_a/Q_c = 94\%$; (5) $|Sb^{III}| = 5 \times 10^{-4}$ M, $|Bi^{III}| = 10^{-3}$ M, $|Sb^{III}|/|Bi^{III}| = 0.50$, $Q_a/Q_c = 93\%$; (6) $|Sb^{III}| = 10^{-3}$ M, $|Bi^{III}| = 10^{-3}$ M, $|Sb^{III}|/|Bi^{III}| = 1$, $Q_a/Q_c = 92\%$; (7) $|Sb^{III}| = 1.2 \times 10^{-3}$ M, $|Bi^{III}| = 10^{-3}$ M, $|Sb^{III}|/|Bi^{III}| = 1.2$, $Q_a/Q_c = 90\%$; and (8) $|Sb^{III}| = 10^{-3}$ M, $Q_a/Q_c = 95\%$.

So the presence of one signal during reduction and oxidation reveals the existence of an electrodeposition process according to the following equation:

$$(1-x)BiCl_4^- + x\,SbCl_4^- + 3\,e^- \rightarrow Bi_{1-x}Sb_x + 4\,Cl^-$$

To confirm this assumption, the anodic voltammogram of a carbon paste reference $Bi_{0.9}Sb_{0.1}$ electrode was recorded in NaCl 4 M + HCl 1 M (Figure 3). The powdered sample synthesized (in the Laboratory of S. Scherrer Laboratoire de Physique du Solide, INPL, Nancy), by directional crystallization was attached to the surface of a glassy carbon rod by means of a colloidal graphite slurry according to a previously described prodedure [20]. A single oxidation peak, with a shape similar to the previous peaks, was detected in the same potential range. The above voltammetric results strongly suggest that a reduction of Sb^{III} and Bi^{III} mixture in a chloride medium is able to induce an alloy electroformation.

3. Electrodeposition of $Bi_{1-x}Sb_x$ films

We concentrated our efforts on a process allowing us to obtain a sufficient bulk film with varying antimony contents. In particular, the electrolyte with a $|Sb^{III}|/|Bi^{III}|$ ratio equal to 0.1 was investigated in order to obtain alloys with an antimony atomic percentage equal to 10%. Indeed, this composition results in the best figure of merit for these thermoelectric materials [17, 18]. Alternative electrochemical strategies were explored for synthesis, namely, potentiostatic and galvanostatic. The former generally leads to deposits with controlled stoichiometry while the latter is commonly used in the electroplating industry.

3.1. *Deposition conditions*

Glassy carbon sheets (Société Carbone Lorraine) were chosen as substrates for the preparation of $Bi_{1-x}Sb_x$ films. The plates were mechanically polished with carborundum paper and with diamond paste (1 μm size). After polishing, the electrodes were cleaned with doubly distilled water followed by p.a grade methanol rinsing. The working electrodes were located horizontally in the bottom of a Teflon cell specially designed in our laboratory. The apparent surface area was equal to 2.0 cm^2. The cathodic polarisation was carried out at room temperature without stirring with a platinum horizontal disk counterelectrode facing the working plate and with a saturated calomel electrode (SCE). The electrochemical cell had an electrolyte volume of 100 ml.

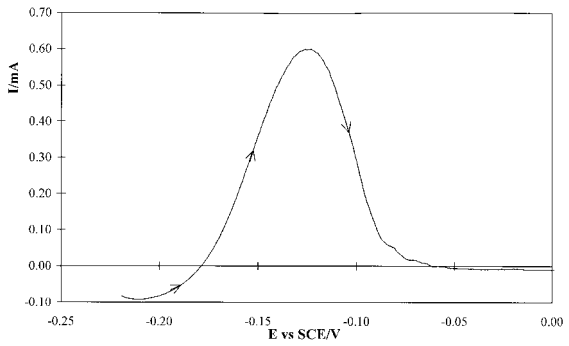

Fig. 3. Anodic oxidation in NaCl 4 M and HCl 1 M of a directionally crystallized $Bi_{0.899}Sb_{0.101}$. Working electrode: glassy carbon, surface area: 7.06 mm^2, scan rate: 60 mV min^{-1}.

The electrolyte composition was imposed by the solubility of Sb^{III} in NaCl 4 M + HCl 1 M. Under these conditions, the concentrations were fixed at 10^{-1} M for Bi^{III} and 5×10^{-3} M to 1×10^{-1} M for Sb^{III} by dissolving $Bi(NO_3)_3.5\,H_2O$ and Sb_2O_3 (analytical grade). The fixed $|Sb|/|Bi|$ ratios (0.052, 0.111, 0.25, 0.5, 0.8, 1) correspond to solutions containing 5, 10, 20, 33, 44.5 and 50 antimony atomic percentage, respectively. Hydrazinium sulfate was added to prevent and neutralise chlorine formation at the counterelectrode (anode). Prior to electrodeposition, the electrolyte was deaerated by argon bubbling during 20 min.

3.2. *Deposit characterizations*

X-ray diffraction data were obtained with a curve detector (INEL, CoK_α radiation). The morphology was studied using a scanning electron microscope (Hitachi, model S 2500 LB). The elemental analyses of the electrodeposited films removed from their supports were performed using two techniques: electron probe microanalysis (Cameca SX 50) calibrated with antimony (purity 99.9%) and Bismuth (purity 99.9%) standards or atomic absorption spectrometry (Solar, Unicam 969). The bismuth and antimony microanalyses were performed in ten different sections of the samples. The stoichiometry corresponds to the average of these ten values and is calculated with a total atom number assigned as 1. Analyses were reproducible within $\pm 1\%$. The stoichiometric determination analyses by AAS were reproducible to 0.5–1%.

The electrical resistivity measurements of the removed films were realized using a van der Pauw technique [21]. Current contacts were made on the underside of sample by soldering copper wires (5 μm) with a colloidal silver slurry.

3.3. *Preparation of films and results*

We studied the influence of electrolysis conditions on the composition and characteristics of antimony–bismuth alloy deposits. In the various electrolytes, the deposition was conducted either at cathodic current densities of -0.4 to -1.0 A dm^{-2} or at potentiostatic polarisations of -300 to -550 mV.

In the potentiostatic process, potentials were applied the time required to obtain films with a thickness equal to 20 μm. It can be seen that the growth rate is varies between 15 (for $|Sb|/|Bi| = 0.0526$ and $E = -300$ mV)

and 60 μm h^{-1} (for $|Sb|/|Bi| = 1$ and $E = -550$ mV). Deposits were gray in color and homogeneous over the electrode surface for $-340\,\text{mV} \leq E_{\text{deposition}} \leq -300$ mV but for a potential less than -340 mV, the deposits were black and pulverulent with a poor adhesion to the electrode surface.

In a galvanostatic process, at higher values (> -1 A dm^{-2}), the films were dark, dull and did not adhere to the glassy carbon electrode. At lower absolute values (-0.4 to -1 A dm^{-2}), deposits of a better quality were obtained with a growth rate between 10 and 25 μm h^{-1}.

The coulombic efficiencies were measured, taking the alloy stoichiometry obtained by the elemental analysis into account, from the mass increase of the electrode after deposition and by comparing the experimental increase to that expected from Faraday's law. For deposits adhering to the electrode, the cathodic current efficiencies was $98 \pm 2\%$ and did not change significantly with electrolyte composition, $E_{\text{deposition}}$, or current density.

Figure 4 shows the variation of the film antimony content as a function of deposition potential and the electrolyte composition. The antimony atomic percentage is not affected by the deposition potential for the lowest antimony concentrations (5, 10 and 20 at % in the electrolyte). The results are different for a solution having a 50 at % ($|Sb|/|Bi| = 1$ in electrolyte). In this latter case, for the more cathodic potentials (-550 to -450 mV), the deposit stoichiometry is close to the electrolyte composition. But for deposits obtained from -400 to -300 mV, an antimony enrichment is observed in the films in comparison with the electrolyte composition. Such results may indicate that the Sb electrodeposition system is very smoothly shifted, in the potential scale, to more positive potential in comparison with that Bi system. The difference can only be observed for the solution having a high antimony content.

The current density dependence of film composition is plotted in Figure 5. The bold line represents a theoritical curve corresponding to the perfect equality between the antimony atomic percentage in the film and in electrolyte.

The atomic ratio of Sb to Bi in the deposits, as determined by AAS or the microprobe, showed a wide

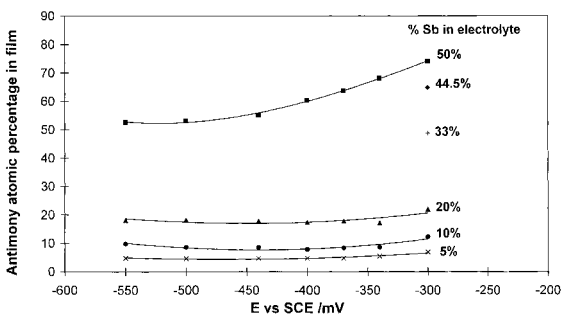

Fig. 4. Evolution of Sb atomic percentage in alloys with deposit potential and electrolyte composition: $|Sb^{III}| = 0.052\,|Bi^{III}|$ (×), $|Sb^{III}| = 0.111\,|Bi^{III}|$ (●), $|Sb^{III}| = 0.250\,|Bi^{III}|$ (▲), $|Sb^{III}| = 0.500\,|Bi^{III}|$ (+), $|Sb^{III}| = 0.80\,|Bi^{III}|$ (◆), $|Sb^{III}| = 1\,|Bi^{III}|$ (■).

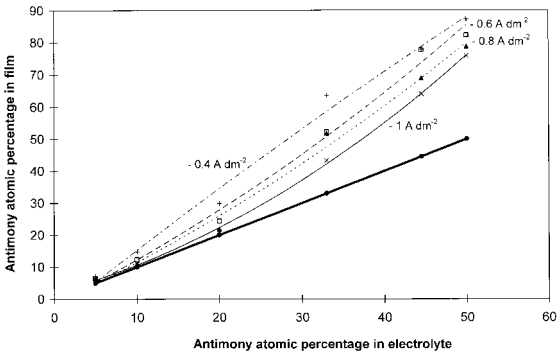

Fig. 5. Alloys stoichiometry *vs* electrolyte composition (both expressed in antimony atomic percentage) at various current densities: (×) 1, (▲) 0.8, (□) 0.6 and (+) 0.4 A dm^{-2}; (●) theoritical curve.

range of compositions accessible by electrochemical deposition. The alloy composition is strongly correlated to the Sb/Bi ratio of the electrolyte. Indeed, the films antimony composition increases with increasing solution ratio, with, however, an antimony content of the deposits generally larger than that fixed by the electrolyte. The difference between the two contents becomes more pronounced for further increases in |Sb| content of the electrolyte. This fact might basically be due to an easier electrodeposition of antimony. Another interesting point to underline is the fact that, for each electrolyte, the antimony percentage of the deposits increases with decreasing cathodic current density. We can conclude from these observations that both systems (Bi^{III}/Bi° and Sb^{III}/Sb°) are always sollicited during electrodeposition since the films are $Bi_{1-x}Sb_x$ alloy phases. However, the results may confirm the above hypothesis: that is, two systems not exactly situated at the same position on the potential scale. Thus, antimony is deposited somewhat preferentially for the lowest current densities.

The X-ray diffraction pattern of films prepared under different cathodic potentials and current densities exhibit a single phase which presents a good crystallinity. For example, that corresponding to a ground sample obtained at -0.4 A dm^{-2} and with an electrolyte having a Sb/Bi ratio equal to 0.1 is shown in Figure 6 and compared with those for Bi° and Sb° and a directionally crystallised $Bi_{0.899}Sb_{0.101}$ compound (from S. Scherrer Laboratory). Examination of the peaks reveals that electrodeposits are not formed from the two separate elements but correspond to a single alloy phase. All the diffraction lines (Table 1) could be completely indexed on the basis of the hexagonal cell or an equivalent rhombohedral one ($R\bar{3}m$). The lattice parameters of the hexagonal structure for all electrodeposits were determined from the observed reticular distances, using a least-squares method. The obtained values were in good agreement with those observed by Ehret et al., Cucka et al. and Dugué et al. [22–24]. The a_h and c_h parameters vary smoothly according to the antimony content of the alloys (Figure 7(a) and (b)). The variation corresponds to a solid solution. It can be noted that

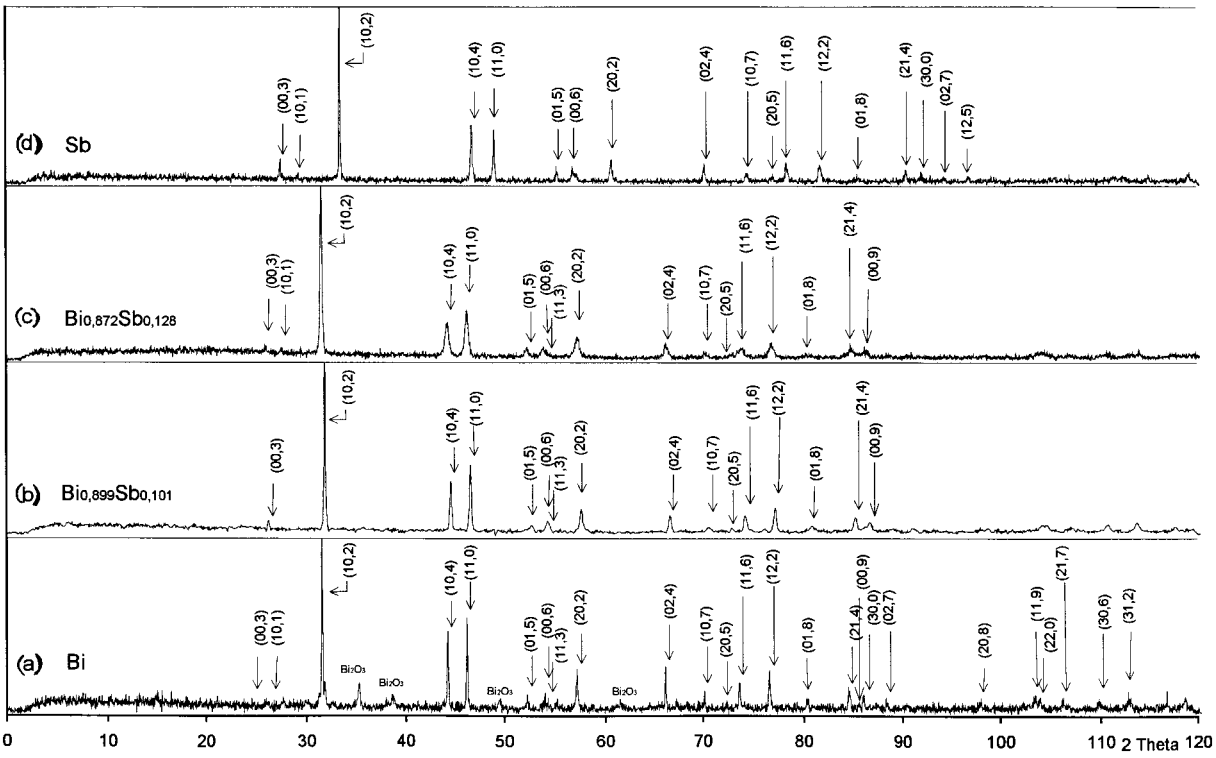

Fig. 6. X-ray powder diffraction diagrams of Bi° (a), $Bi_{0.899}Sb_{0.101}$ obtained by directional crystallisation (b), $Bi_{0.872}Sb_{0.128}$ electrodeposit obtained under galvanostatic conditions ($i = -0.4$ A dm^{-2}, $|Sb^{III}| = 0.111|\ Bi^{III}|$), (c) and Sb°.

for bulk deposits, the intensity ratios of peaks are not in good agreement with those obtained on a ground product. This fact indicates an orientational effect in the film growth. A full explanation of this behaviour will require further texture studies.

The examination of samples by SEM reveals that their surface is covered by crystallites, agglomerated in polycrystalline nodules exhibiting growth steps. The morphology of the alloy deposits depends on their chemical composition. It has been found that a fine-grained structure is observed for the films electrodeposited from an electrolyte containing an antimony atomic percentage equal to 5% (Figure 8(a)). Above this composition, the deposit structure becomes coarser (Figure 8(b) and (c). However, as the electrolyte antimony content increases from 10 to 50%, the crystallite size decreases and the surface relief of the deposits becomes smoother (Figure 8(d)). Moreover, the cathodic current density is an important factor influencing the crystallite size. It becomes larger as the applied density is increases.

The resistivity measurements were made to determine the influence of the electrolysis conditions and the composition of samples. All the films peel off from the glassy carbon substrate after the electrodeposition. This characteristic presents an advantage for the electrical measurements of the films. The four-point d.c. probe method shows that the prepared films have resistivities in the 3–7 $\mu\Omega$ m range (Figure 9). These values are slightly larger than that of a single crystal (2 $\mu\Omega$ m) [4, 17]. This may be owing to large grain boundary discontinuities in electrodeposited films. A remarkable finding arises from examination of the resistivity evolution as a function of the antimony content of the films. A common feature is the shape of the curves whatever the applied current density. As the antimony atomic ratio raises from 5 to 20%, the resitivity increases. Relatively larger resistivities have been observed for the deposited film having a 20% antimony content. Above this ratio, the resistivity continuously decreases and a stabilization at 3.5 $\mu\Omega$ m is observed for the richest antimony alloys. Another striking fact is that the maximum resistivities correspond to the deposits obtained with the highest current density. These observations can be ascribed to the change in the films morphology. We have seen from SEM observations that the current density and the chemical composition can influence the grain size of the films. Smooth deposits of the highest quality were obtained for -0.4 A dm^{-2} and for the two extreme compositions. Such results may indicate the predominance of the film roughness in determining the resistivity value. Coarser films with a significant roughness have higher resistivity values than those with a smoother structure probably allowing a better electronic mobility.

4. Conclusion

A novel electrolyte (NaCl 4 M and HCl 1 M) has been used to form electrodeposits of bismuth and antimony

Table 1. Comparison of X-ray diffraction peaks from Figure 6 with those for Bi°, Sb° and an alloy prepared by directional crystallization

ASTM	Bi	44-1246	Experimental $Bi_{0.899}Sb_{0.101}$ (ref.)			ASTM	Sb	35-732	Experimental $Bi_{0.872}Sb_{0.128}$		
d/Å	*i*	*h k.l*	*d*/Å	*i*	*h k.l*	*d*/Å	*i*	*h k.l*	*d*/Å	*i*	*h k.l*
3.954	6	0 0.3									
			3.942	3.8	0 0.3				3.95	3.20	0 0.3
						3.753	25	0 0.3			
			missing						3.74	2	1 0.1
3.737	2	1 0.1									
						3.538	4	1 0.1			
3.280	100	0 1.2									
			3.265	100	0 1.2				3.278	100	0 1.2
						3.109	100	0 1.2			
2.369	27	1 0.4									
			2.537	46	1 0.4				2.362	45	1 0.4
2.273	29	1 1.0									
			2.260	52.6	1 1.0				2.265	49.2	1 1.0
						2.248	70	1 0.4			
						2.152	56	1 1.0			
2.032	5	0 1.5									
			2.019	4.7	0 1.5				2.024	10.7	0 1.5
1.977	6	0 0.6									
1.971	6	1 1.3									
			1.964	9.9	0 0.6				1.967	11.3	0 0.6
			1.958	4.6	1 1.3				1.957	1.2	1 1.3
1.942	1	0 2.1									
						1.929	12	0 1.5			
						1.878	35	0 0.6			
1.869	13	2 0.2									
			1.857	25.2	2 0.2				1.859	29.1	2 0.2
						1.770	26	2 0.2			
1.640	7	0 2.4									
			1.630	14.5	0 2.4				1.631	19.2	0 2.4
1.557	3	1 0.7									
						1.555	15	0 2.4			
			1.548	2.4	1 0.7				1.547	4.5	1 0.7
1.515	1	2 0.5									
1.492	8	1 1.6									
			1.482	20.6	1 1.6				1.483	19.2	1 1.6
						1.479	13	1 0.7			
1.477	1	2 1.1									
1.444	10	1 2.2									
						1.437	12	2 0.5			
			1.434	24.9	1 2.2				1.434	19	1 2.2
						1.416	63	1 1.6			
1.388	2	0 1.8									
			1.380	11	0 1.8				1.380	4.9	0 1.8
						1.368	67	1 2.2			
1.330	5	2 1.4									
			1.322	18.5	2 1.4				1.322	16.7	2 1.4
1.318	1	0 0.9				1.318	30	0 1.8			
1.313	2	3 0.0									
			1.304	15.2	0 0.9				1.306	10.5	0 0.9
1.284	1	0 2.7									
1.261	1	1 2.5				1.261	40	2 1.4			
						1.252	25	0 0.9			
1.246	1	3 0.3									
						1.243	30	3 0.0			
						1.219	11	0 2.7			
						1.196	12	1 2.5			
1.184	1	2 0.8									
						1.180	5	3 0.3			

alloys. The analytical study of the reduction of Bi^{III}, Sb^{III} and their mixtures has established the direct electroformation of alloys. By controlling the electrode potential, the current density or the electrolyte composition, it is possible to achieve a large range of antimony to bismuth composition ratios in the deposits. The electrodeposited films, corresponding to a solid solution, are polycrystalline. The grain size is influenced by the electrolyte composition and the current density. There is a good correlation between the resistivity data and the morphology of the films.

Further work will focus on the characterization of the semiconductive and thermoelectric properties of $Bi_{1-x}Sb_x$ layers.

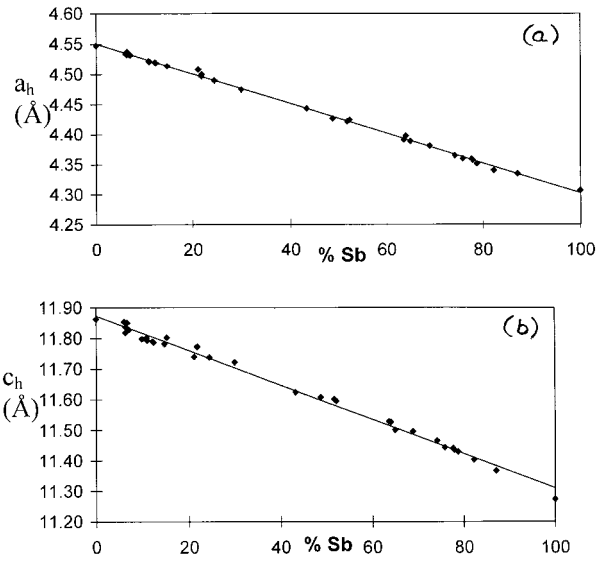

Fig. 7. Hexagonal a_h (a) and c_h (b) lattice parameters of electrodeposited films against antimony atomic percentage.

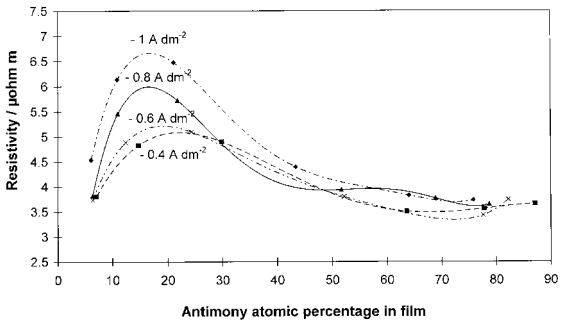

Fig. 9. Resistivity dependence on alloy stoichiometry at various current densities.

Acknowledgements

The authors are indebted to Dr J.J. Heizmann and Dr B. Bolle of Letam–Isgmp (Metz) for recording X-ray diffractograms and to A. Kohler of Service Commun de Microanalyse (Nancy I) for the SEM experiments.

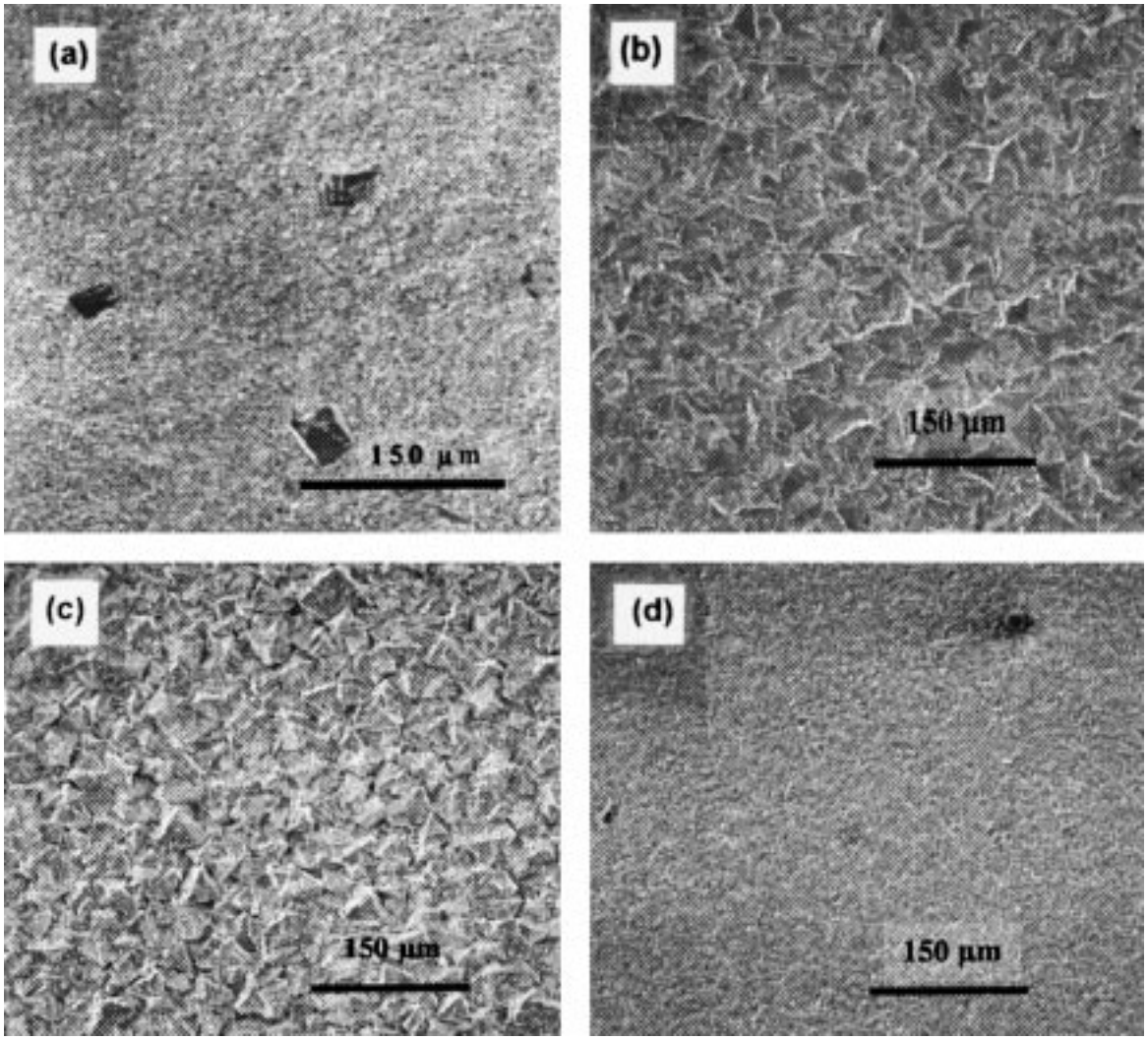

Fig. 8. SEM photographs of $Bi_{1-x}Sb_x$ films deposited onto a glassy carbon substrate, $i = -0.4$ A dm^{-2}, at various antimony atomic percentages in electrolyte: (a) 5%, (b) 10%, (c) 20 and (d) 50%.

References

1. G.E. Smith and R. Wolfe, *J. Appl. Phys.* **33** (1962) 841.
2. W.M. Yim and A. Amith, *Solid State Electron*, **15** (1972) 1141.
3. M.A. Short and J.J. Schott, *J. Appl. Phys.* **36** (1965) 659.
4. B. Lenoir, A. Demouge, D. Perrin, H. Scherrer, S. Scherrer, M. Cassart and J.P. Michenaud, *J. Phys. Chim. Solids* **56** (1995) 99.
5. R. Martin-Lopez, M. Zandona and H. Scherrer, *J. Mater. Sci. Lett.* **15** (1996) 16.
6. P. Panicker, F.A. Kröger and M. Castner, *J. Electrochem. Soc.* **125** (1978) 566.
7. C. Lokhande and S. Pawar, *Phys. Status Solidi A* **111** (1989) 17.
8. C. De Mattei and R. Feigelson, *in* 'Electrochemistry of Semiconductors and Electronics: Process and Devices', edited by J. Mc Hardy and F. Ludwig (Park Ridge, NJ, 1992), p. 1.
9. A.D. Styrkas, V.V. Ostroumov and G.V. Anan'eva, *Zh. Prikl. Khim.* **37** (1964) 2431.
10. Y.N. Sadana and J.P. Singh, *Plat. Surf. Finish.* **64** (1985) 64.
11. Y.N. Sadana, J.P. Singh and R. Kumar, *Surf. Tech.* **24** (1985) 315.
12. F. Paolucci, G. Mengoli and M. Musiani, *J. Appl. Electrochem.* **20** (1990) 868.
13. V. Povetkin, T. Shibleva and M. Kovenskii, *Elektrokhimiza* **26** (1990) 1616.
14. A. Jain, *Phys. Rev.* **114** (1959) 1518.
15. S. Golin, *Phys. Rev.* **176** (1968) 830.
16. N. Brandt, R. Hermann, R. Golysheva, L. Devyatkova, D. Kusnik, W. Kraak and Y. Ponomarev, *Sov. Phys. JETP* **56** (1982) 1247.
17. B. Lenoir, PhD thesis, INPL, Nancy, France (1994).
18. B. Lenoir, M. Cassart, J.P. Michenaud, H. Scherrer and S. Scherrer, *J. Phys. Chem. Solids* **57** (1996) 89.
19. 'Encyclopedia of Electrochemistry of the Elements', Vol IV and Vol IX Part B, edited by A. Bard, Marcel Dekker, (New York Basel, 1975).
20. C. Boulanger and J.M. Lecuire, *Electrochim. Acta* **32** (1987) 345.
21. L. Van der Pauw, *Philips Res. Reports* **13** (1958) 1 and **20** (1958) 220.
22. W.F. Ehret and M.B. Abramson, *J. Am. Chem. Soc.* **56** (1934) 385.
23. P. Cucka and C.S Barett, *Acta Cryst.* **15** (1962) 865.
24. M. Dugué, *Phys. Status Solidi* **11** (1965) 149.